Downloaded from jnm.snmjournals.org by Ronald Lattanze on February 13, 2020. For personal use only.

2018 SNMMI Highlights Lecture: General Nuclear Medicine

Heather A. Jacene, MD, Dana-Farber Cancer Institute, Brigham and Women's Hospital, and Harvard Medical School, Boston, MA

From the Newsline Editor: The Highlights Lecture, presented at the closing session of each SNMMI Annual Meeting, was originated and presented for more than 30 years by Henry N. Wagner, Jr., MD. Beginning in 2010, the duties of summarizing selected significant presentations at the meeting were divided annually among 4 distinguished nuclear and molecular medicine subject matter experts. Each year Newsline publishes these lectures and selected images. The 2018 Highlights Lectures were delivered on June 26 at the SNMMI Annual Meeting in Philadelphia, PA. In this issue we feature the lecture by Heather A. Jacene, MD, associate professor in the Department of Radiology at Dana-Farber Cancer Institute, Brigham and Women's Hospital, and Harvard Medical School (Boston, MA), who spoke on highlights in general nuclear medicine. Note that in the following presentation summary, numerals in brackets represent abstract numbers as published in The Journal of Nuclear Medicine *(2018;59[suppl 1]).*

I am delighted to present the General Nuclear Medicine highlights at the 2018 SNMMI Annual Meeting. The General Clinical Specialties track this year featured 210 abstracts, covering the breadth of nuclear medicine, including but not limited to somatostatin receptor scintigraphy, musculoskeletal, gastroenterology, thyroid and parathyroid, pediatrics, renal/hypertension, and outcomes/infection/pulmonary topics. Because of an overlap in subject matter with therapy, somatostatin receptor scintigraphy will be covered in the Oncology Highlights presentation.

Posters and podium presentations at this meeting represented practices from around the world. In the General Clinical Specialties, however, approximately 75% of abstracts came from the United States or China. Several common themes emerged during my review of the abstracts in the General Clinical Specialties track, including foci on efficiency, quantitation, development, and outcomes. I selected abstracts that were representative of each of these categories and organized this presentation along these themes. I want to thank all of the authors who generously sent slides, and I regret that the limited lecture time does not allow me to show all of the excellent work that was presented at this meeting.

Efficiency

Most of the abstracts addressing this theme focused on time and dose efficiency, and the balance on image quality and accuracy. Similar to advances in PET development, instrumentation for general nuclear medicine also continues to evolve. Yamane et al. from Saitama Medical University Hospital (Iruma-gun), Saitama Medical University International Medical Center (Hidaka), and Tokyo Metropolitan University (all in Japan) reported on "Ultrafast bone scan by the use of cadmium-zinc-telluride (CZT) whole-body gamma camera" [112]. The authors looked at 64 patients (42 male, 22 female) who underwent bone scintigraphy for detection of bone metastases from prostate cancer (n = 31), lung cancer (n = 18), breast cancer (n = 12), and hepatocellular carcinoma (n = 3). Images were acquired with a novel whole-body SPECT/CT scanner with CZT detectors that use list-mode data acquisition. After the acquisition of list-mode data for 180 seconds per bed position, anterior and posterior whole-body images were reconstructed using 5%, 10%, 25%, 50%, 75%, and 100% of the list-mode data. Figure 1 shows that, as the calculated time diminished, image quality remained reasonably good, down into the 25%–10% range. The authors looked at 3 different values for autoquantitation: bone scan index, artificial neural network, and hotspot number. For the bone scan index, quantitative indices for short-time acquisition generally corresponded to the 100% image, even at 10% of the scan time. The images were somewhat more degraded at the 5% time point. Interclass correlation coefficients were excellent down to 10%. The authors concluded that the "whole-body CZT camera has the potential to reduce scan time or the injection dose of the radioisotope to evaluate the bone scan index of bone scan."

Heather A. Jacene, MD

In a study with similar dose reduction–focused goals, Schmall et al. from the Children's Hospital of Philadelphia (PA) and the University of Pennsylvania (Philadelphia) reported on "Investigating low-dose image quality in pediatric time-of-flight (TOF) PET/MRI" [304]. The study characterized the quantitative accuracy of ^{18}F-FDG uptake for simulated low-dose imaging studies and investigated associated improvements with TOF PET reconstruction. The study was performed with a combination of phantom imaging and retrospective clinical data from pediatric patients with metastatic liver lesions who underwent PET/MR imaging. The authors then simulated low-dose images from subsampled datasets. The first image on the left in Figure 2 is the clinical image, followed by the simulated results at (left to right) 1/2-, 1/3-, 1/6-, and 1/9-dose decrements. Image quality remained quite good down to 1/2 dose and even 1/3 dose, with liver SUVs maintained down to 1/3 dose. In a smaller interreader study, experienced readers

Downloaded from jnm.snmjournals.org by Ronald Lattanze on February 13, 2020. For personal use only.

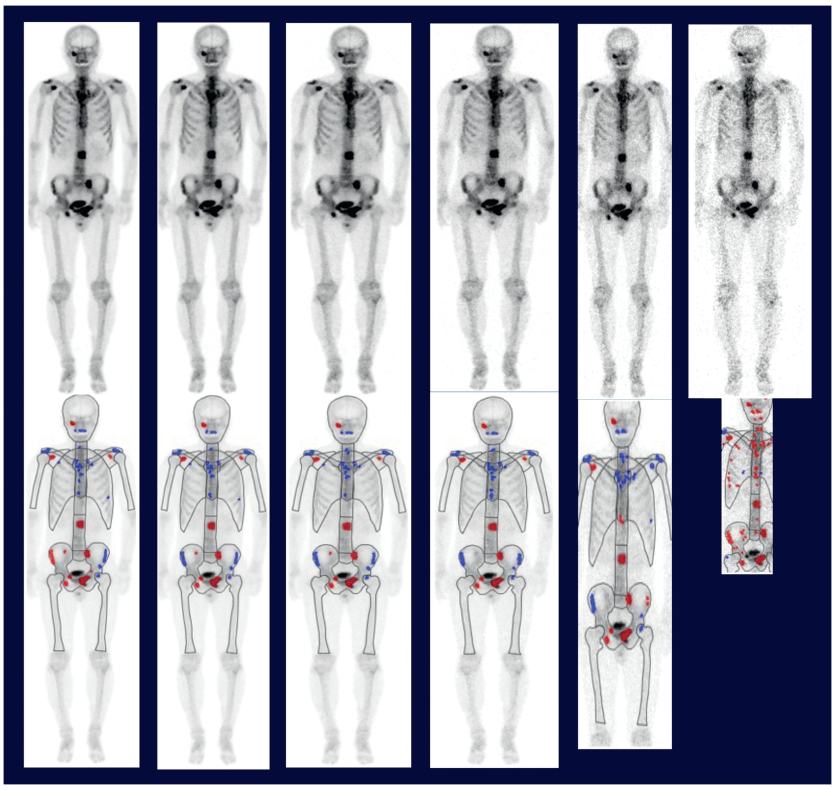

FIGURE 1. Ultrafast bone scanning with CZT whole-body gamma camera. Reconstructed images in a cancer patient acquired at (left to right): 100% (bone scan index [BSI] = 2.3), 75% (BSI = 1.98; interclass correlation [ICC] = 0.97), 50% (BSI = 1.90; ICC = 0.97), 25% (BSI = 2.05; ICC = 0.95), 10% (BSI = 2.30; ICC = 0.95), and 5% (BSI = 4.62; ICC = 0.84) of the original clinical scan time. Results showed that autoquantitation with the whole-body CZT camera has the potential to reduce scan time and/or injected dose.

rated visual image quality on a Likert scale, and the results indicated that, at 1/2 and 1/3 of the dose, image quality was like that of full-dose images. No performance degradation was observed at 1/2-dose levels, so that dose reduction appears to be feasible for pediatric patients with TOF PET/MR imaging, and further reduction may be possible with optimized PET reconstruction and MR imaging.

Quantitation

Quantitation remains an area of interest in general nuclear medicine. Software is now available to provide SPECT SUVs, accompanied by many efforts to identify and validate clinical applications. Bae and Lee from Seoul National University Bundang Hospital (Seongnam) and Seoul National University Hospital (Seoul, both in the Republic of Korea) reported on "Maximum SUV of foot SPECT/CT using ^{99m}Tc-hydroxymethylene phosphonate (^{99m}Tc-HDP) in patients with accessory navicular bone as a predictor of surgical treatment" [115]. The premise of this retrospective observational study was to determine whether quantitative SPECT/CT could be used to differentiate types of accessory navicular bone that cause symptoms and necessitate surgical management versus types that do not and can be treated conservatively. Figure 3 is a typical example of a symptomatic accessory navicular bone on (left to right) SPECT/CT, bone scan, and SPECT.

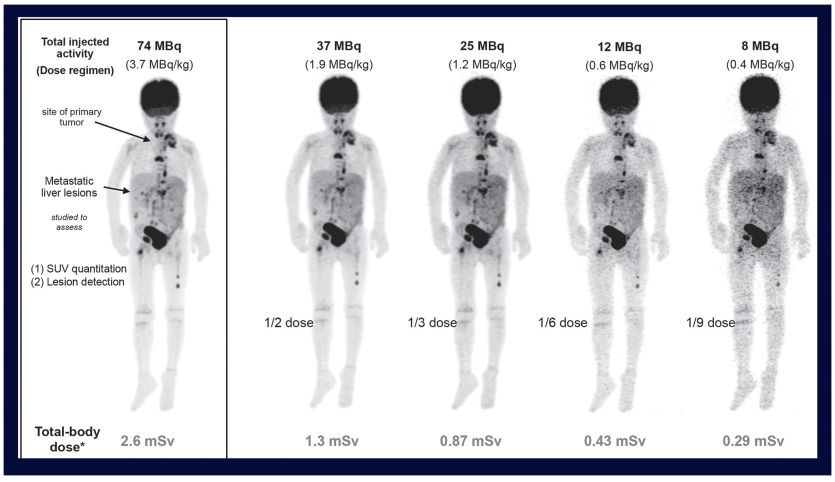

FIGURE 2. Enhancing pediatric time-of-flight (TOF) PET/MR reconstruction. The original clinical scan is at left (total body dose [TBD] = 2.6 mSv; total injected activity/dose regimen [TIA/DR] = 74 MBq/3.7 MBq/kg), followed by simulated low-dose images from subsampled data (left to right) for: 1.3 mSv TBD (1/2 dose; TIA/DR = 37 MBq/1.9 MBq/kg), 0.87 mSv TBD (1/3 dose; TIA/DR = 25 MBq/1.2 MBq/kg); 0.43 mSv TBD (1/6 dose; TIA/DR = 12 MBq/0.6 MBq/kg), and 0.29 TBD (1/9 dose; TIA/DR = 8 MBq/0.4 MBq/kg). The authors concluded that pediatric imaging at 1.9 MBq/kg, half of the North American Consensus Guidelines, is feasible with TOF-PET/MR reconstruction.

Downloaded from jnm.snmjournals.org by Ronald Lattanze on February 13, 2020. For personal use only.

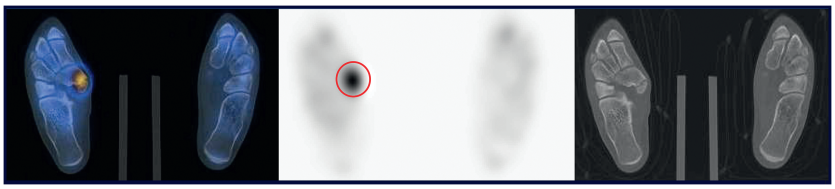

FIGURE 3. ^{99m}Tc-hydroxymethylene phosphonate SPECT/CT in accessory navicular bone (ANB) classification. Shown is an example of a patient with a symptomatic right accessory navicular bone on (left to right): SPECT/CT, bone scan, and SPECT. SUV_{max} on SPECT/CT was higher in the subgroup of patients with type 2-1 ANB, and these patients were more likely to proceed to surgery. If further validated, quantitative SPECT/CT SUV could help guide decision making for surgical management in ANB.

A total of 105 individuals with foot pain were divided into 2 groups: 31 controls without accessory navicular bone and 74 accessory navicular bone patients with unilateral ($n = 7$) or bilateral ($n = 67$) involvement. Involvement was classified into type 1, 2, or 3 (Geist classification), and type 2 patients were subclassified into 2-1 (with subchondral cortical irregularities or degenerative change) or 2-0 (without such bony abnormality). On ^{99m}Tc-HDP imaging, SUV_{max} was significantly higher in the type 2-1 group than in other types of accessory navicular bone, normal controls, or the contralateral foot in individuals with a unilateral accessory navicular bone. Type 2-1 patients were also more likely than other groups to proceed to surgery. The authors concluded that quantitative bone SPECT/CT is useful for disease classification in this setting and that SUV_{max} may aid in risk stratification to suggest the need for surgical therapy. The results of this study are promising and should be validated in a prospective study to assess impact on surgical management and decision making.

As part of the nicely named PERF-ECT trial, Nicolas et al. from University Hospital Basel (Switzerland), Siemens Healthcare GmbH (Forchheim, Germany), and Siemens Medical Solutions USA, Inc. (Hoffman Estates, IL) reported on "Quantitative and anatomical assessment of lung perfusion with ^{99m}Tc-macroaggregated albumin (^{99m}Tc-MAA) SPECT/CT in emphysema and lung cancer patients" [516]. This was a single-center prospective study of 112 patients with varying types of cardiopulmonary disease. The study was a head-to-head comparison of 2D and 3D ^{99m}Tc-MAA perfusion quantification, designed to assess interobserver variability as well as to test the accuracy of the 2D and 3D methods with an anthropomorphic phantom as the gold standard (Fig. 4). The researchers found that interobserver variability was greater for the 2D oblique method than for the 3D SPECT/CT quantitative method. This was also confirmed by interclass correlation coefficients, which were much higher for the 3D method (0.986) than the 2D oblique method (0.860). At the lobar level, a significant difference was identified between the 2 methods. Although the 2D method underestimated the contribution of the upper lobes, the lower lobes were consistently overestimated compared to the 3D method. The 3D method was closer to the gold standard for accuracy than the 2D method. This is clinically relevant, because many of these patients undergoing quantitative lung scans are being assessed for surgical management, and this quantitation can contribute to decision making on surgical versus nonsurgical status. The authors concluded that 3D quantification of lung perfusion is feasible in clinical practice, shows substantial incongruity to the routinely used 2D method at the lobar level, and yields excellent interobserver agreement, warranting additional studies to assess its clinical value, especially in predicting postoperative outcomes.

Development

Research and development in general nuclear medicine are alive and well. New tracers are being developed at the same time that novel applications are being identified for old tracers. The group from Emory University (Atlanta, GA) has a long history of developing agents for renal scintigraphy, and, at this meeting, Lipowska et al. reported on "Initial evaluation of ^{99m}Tc(CO)$_3$-*N*-(2-acetamido)iminodiacetate [^{99m}Tc(CO)$_3$(ADA)]) as a new renal tubular tracer in normal volunteers" [1587]. Earlier data on this new tracer in rats suggested that its pharmacokinetic properties were essentially identical to those of ^{131}I-OIH (hippuran). The objective of this study was to compare the pharmacokinetic properties of ^{99m}Tc(CO)$_3$(ADA) with those of ^{131}I-OIH in normal humans. The image quality was

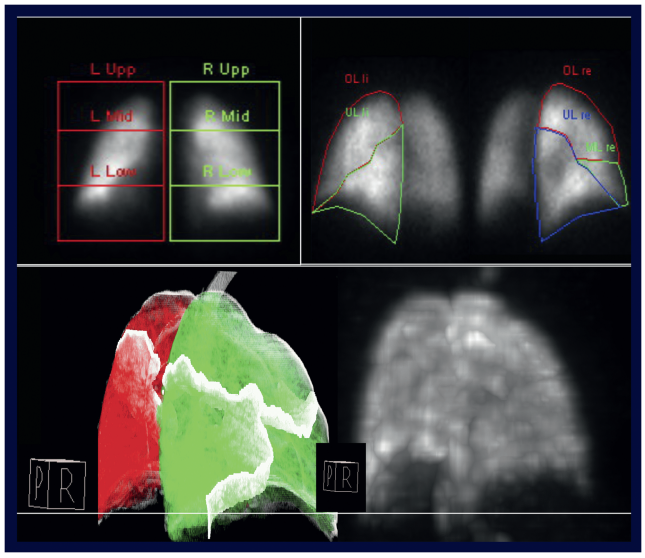

FIGURE 4. Quantitative and anatomic assessment of lung perfusion with ^{99m}Tc-macroaggregated albumin SPECT/CT, comparing 2D and 3D perfusion quantification. The investigators concluded that 3D quantification of lung perfusion is clinically feasible, with excellent interobserver agreement and the potential to predict postoperative outcomes.

Downloaded from jnm.snmjournals.org by Ronald Lattanze on February 13, 2020. For personal use only.

a little better with ^{99m}Tc(CO)$_3$(ADA), as expected, but the time–activity curves of the 2 agents were quite similar. The new agent had slower clearance than ^{131}I-OIH; however, ^{99m}Tc(CO)$_3$(ADA) had a better clearance rate than ^{99m}Tc-mercaptoacetyltriglycine (^{99m}Tc-MAG3), which most of us are currently using in our clinics. The authors concluded that ^{99m}Tc(CO)$_3$(ADA) demonstrated rapid renal extraction and high specificity for renal excretion, despite lacking the negative-charged pendant carboxyl group long considered essential for tubular transport. Their preliminary data suggested that plasma clearance of ^{99m}Tc(CO)$_3$(ADA) is substantially greater than that of ^{99m}Tc-MAG3 but slightly less than that of ^{131}I-OIH. Not only have they developed a new agent, but their results also challenge some of the old paradigms of chemistry in general nuclear medicine. This study was awarded the first prize for poster presentations in General Clinical Specialties at this meeting.

In a very creative study, Osayande et al. from the University of the Witwatersrand (Johannesburg, South Africa) asked "Lung ventilation scintigraphy—What is the ideal radioaerosol?" [1616]. At a time when it appeared possible that these authors and others in their region would not have available supplies of diethylenetriamine pentaacetic acid (DTPA) for imaging agents, they devised a study to look for alternatives for use in lung ventilation scintigraphy. A total of 129 patients with suspected pulmonary embolism with normal chest radiography who were not debilitated were prospectively included. Patients were randomized to undergo imaging with aerosolized ^{99m}Tc-DTPA, ^{99m}Tc-methyldiphosphonate (^{99m}Tc-MDP), or ^{99m}Tc-sestamibi (^{99m}Tc-MIBI). Alveolar clearance was visually assessed in a blinded reader evaluation. Alveolar clearance was also assessed using a semiquantitative method. The authors showed that ^{99m}Tc-MIBI produced generally better image quality, slower alveolar clearance, and higher count rates than the other 2 tracers, with significantly better image quality than ^{99m}Tc-DTPA. Moreover, fewer patients in the ^{99m}Tc-MIBI group had bronchial/tracheal and stomach activity visualized than in the ^{99m}Tc-MDP and ^{99m}Tc-DTPA groups. Figure 5 shows example images with all 3 tracers. Note the central deposition in the stomach as routinely seen on the ^{99m}Tc-DTPA image that is not seen with either of the other 2 tracers. The authors concluded by recommending that either ^{99m}Tc-MIBI or ^{99m}Tc-MDP can replace ^{99m}Tc-DTPA as clinically and economically needed. This shows that when we are short of a radiotracer, it is possible to be creative and prospectively assess alternatives that may already be in use for other applications.

Chen et al. from the Hong Kong Sanatorium and Hospital reported on "^{177}Lu-DOTATATE radionuclide therapy for pediatric patients with relapsed high-risk neuroblastoma negative on ^{131}I-MIBG imaging—A pilot study" [307]. Six children with Neuroblastoma Staging System stage IV and relapsed disease were enrolled and underwent both ^{131}I-MIBG scintigraphy and ^{68}Ga-DOTATATE PET/CT to evaluate their pretreatment disease status in terms of lesion detection sensitivity and tracer avidity. In this first part of the study, the researchers demonstrated that in patients with ^{131}I-MIBG–negative disease ^{68}Ga-DOTATATE scans were positive, showing multiple lesions. This has clinical relevance, because these results suggest a new target for treatment. The patients went on to receive ^{177}Lu-DOTATATE therapy, with a response to therapy shown in Figure 6. The authors also demonstrated safe dosimetry in this pediatric population. This provides preliminary data for future studies that have the potential to open up indications for ^{177}Lu-DOTATATE therapy in children.

Outcomes and Quality Improvement

A number of studies presented in the General Clinical Specialties category at this meeting looked at outcomes and quality improvement across the spectrum of care and practice. Dibble et al. from Brown University/Rhode Island Hospital (Providence) asked "FDG PET/CT imaging of infection: Should it replace labeled leukocytes in inpatients with suspected infection?" [442]. The study included 183 patients from 2009 to 2017 who underwent either radiolabeled white blood cell (WBC; $n = 81$) or ^{18}F-FDG PET/CT ($n = 102$) imaging. The first aim was to assess the sensitivity, specificity, and "helpfulness" to referring clinicians of radiolabeled WBC scans compared to ^{18}F-FDG-PET/CT scans in inpatients with suspected infection. The authors also assessed the number of radiolabeled WBC and ^{18}F-FDG PET/CT scans performed in inpatients with suspected infection

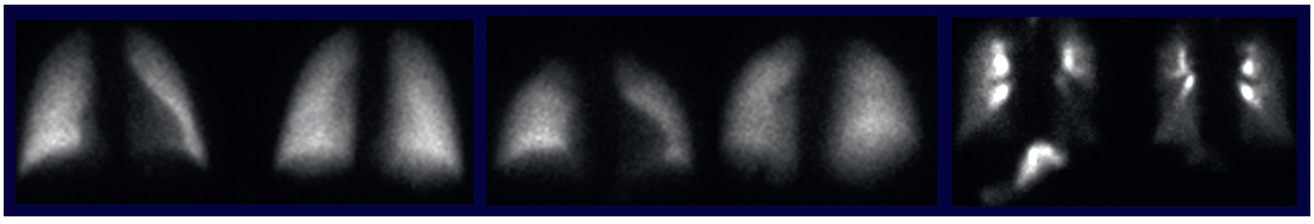

FIGURE 5. Evaluating lung ventilation scintigraphy alternatives in a diethylenetriamine pentaacetic acid (DTPA) distribution shortage. Images with alternative agents were acquired in randomized patients with suspected pulmonary embolism and normal chest radiography. Sample images are shown with aerosolized ^{99m}Tc-methyldiphosphonate (^{99m}Tc-MDP, left), ^{99m}Tc-sestamibi (^{99m}Tc-MIBI, middle), and ^{99m}Tc-DTPA (right). ^{99m}Tc-MIBI produced generally better image quality and slower alveolar clearance, although the investigators concluded that either ^{99m}Tc-MIBI or ^{99m}Tc-MDP can replace ^{99m}Tc-DTPA as needed. Note the central tracer deposition in the stomach as routinely seen on ^{99m}Tc-DTPA imaging but not seen with the other 2 tracers.

Downloaded from jnm.snmjournals.org by Ronald Lattanze on February 13, 2020. For personal use only.

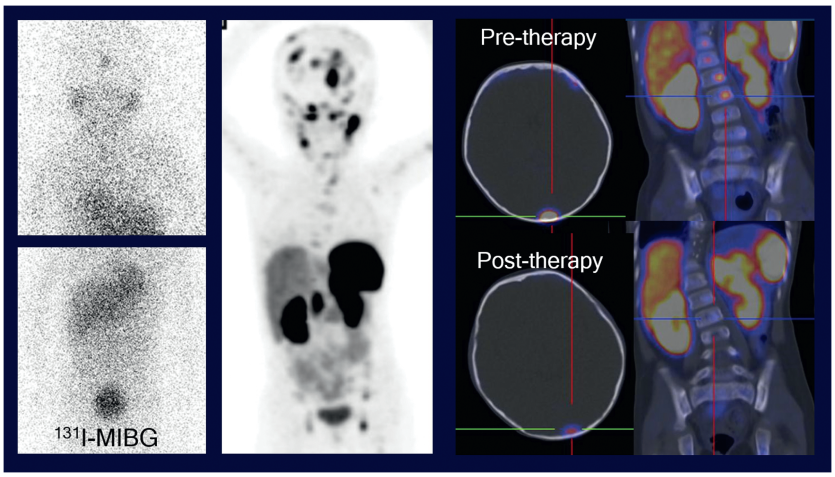

FIGURE 6. ^{177}Lu-DOTATATE radionuclide therapy for pediatric patients with relapsed high-risk neuroblastoma negative on ^{131}I-MIBG imaging (left block) but positive on pretreatment ^{68}Ga-DOTATATE PET/CT (right block). ^{131}I-MIBG imaging (left) showed increased uptake in the skull whereas many more lesions were seen on the ^{68}Ga-DOTATATE-PET/CT (middle). ^{68}Ga-DOTATATE-PET/CT after therapy showed a decrease in somatostatin receptor expression (right two panels).

over the 9-year period and looked at the relative radiopharmaceutical costs for radiolabeled WBC and ^{18}F-FDG-PET/CT. Sixty-one patients were excluded from the PET group because imaging was not performed for infectious indications, and 24 patients from the WBC scan group were excluded because their images included only a section of the body (i.e., were not whole-body scans). Both sensitivity and positive predictive values were higher in the ^{18}F-FDG PET/CT group. The investigators also found that with a positive report, the odds of being helpful to referring clinicians increased 4.6-fold for ^{18}F-FDG PET/CT vs WBC scans, whereas a negative report did not result in any difference in observed helpfulness between the 2 imaging approaches. Figure 7 is one example of a "helpful" ^{18}F-FDG PET scan. The patient was admitted with bacteremia, fever, and low back pain. Targeted MR imaging of the low back (left) was completely negative. About one week later, the patient remained febrile, with no identified source of infection. Whole-body ^{18}F-FDG PET/CT imaging (E,G) showed focal uptake at the L5-S1 epidural space. This allowed physicians to target the next set of diagnostic studies (A,B,D,H) to that area, by which time an epidural abscess had developed on MR imaging (Fig. 7H arrows). ^{18}F-FDG PET imaging visualized the findings earlier than MR imaging and aided in guiding therapy in this patient. In looking at the costs of the 2 imaging techniques, radiolabeled WBCs became more expensive over the study period, whereas the cost of ^{18}F-FDG decreased. By 2017, the cost of a dose of labeled WBCs was 10 times that of a dose of ^{18}F-FDG. The authors concluded that ^{18}F-FDG PET/CT imaging is sensitive and helpful for evaluating suspected infection in the inpatient setting and often can be completed more quickly and without the use of blood products. Additional insights from the study (which was not a head-to-head comparison) suggested that such analyses can be used not only to assess how different technologies and agents affect clinical care but also to enhance knowledge about cost effectiveness.

Antwi et al. from University Hospital Basel (Switzerland) and the University of Basel Hospital (Freiburg, Germany) reported on "Comparison of glucagon-like-peptide-1 (GLP-1) receptor PET/CT, SPECT/CT, and 3T MRI for the localization of occult insulinomas: Evaluation of accuracy in a prospective crossover imaging study" [44]. This was a single-arm prospective study. The final group of 38 patients enrolled had neuroglycopenic symptoms as a result of endogenous hyperinsulinemia hypoglycemia and no evidence for metastatic disease on conventional imaging. All underwent ^{68}Ga-DOTA-exendin-4 PET/CT, ^{111}In-DOTA-exendin-4 SPECT/CT, and standardized 3T contrast-enhanced MR imaging in a random crossover study within a 5-day period. (Simply acquiring these studies in this group of patients in such a limited time period was a remarkable feat.)

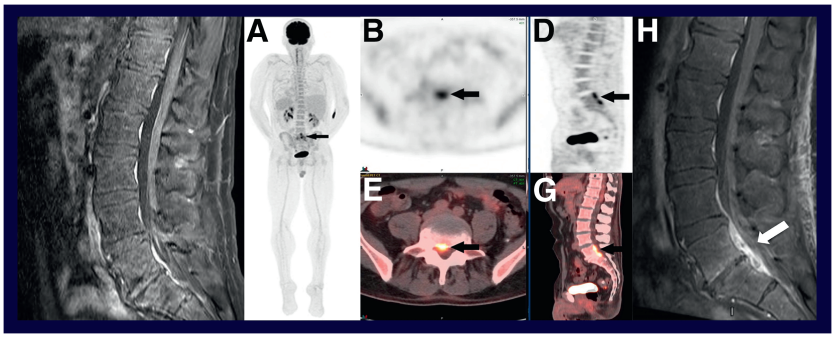

FIGURE 7. ^{18}F-FDG PET/CT versus radiolabeled white blood cell scanning in suspected infection. Shown is an example of a PET scan that was diagnostically helpful. The patient was admitted with bacteremia, fever, and low back pain. Targeted MR imaging of the low back (left) was negative. About one week later the patient remained febrile, with no identified source of infection. Whole-body PET/CT imaging (A,B,D,E,G) showed focal uptake at the L5-S1 epidural space. This allowed physicians to target the next set of diagnostic studies (A,B,D,H) to that area, by which time an epidural abscess had developed (arrows).

Downloaded from jnm.snmjournals.org by Ronald Lattanze on February 13, 2020. For personal use only.

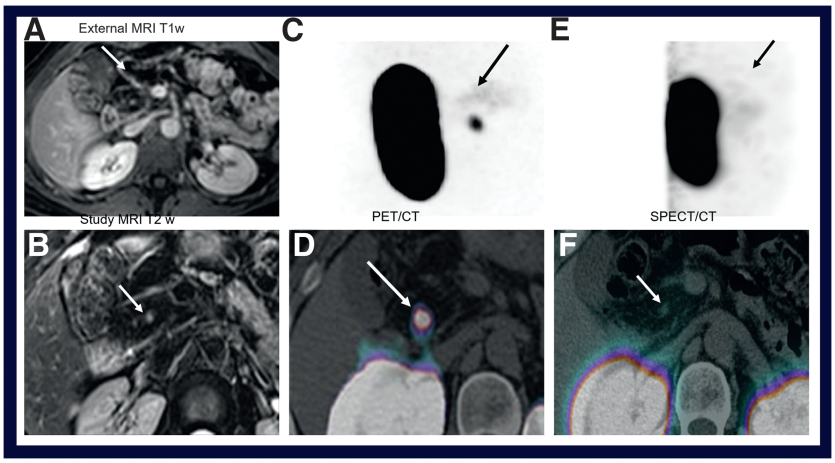

FIGURE 8. Comparison of ^{68}Ga-DOTA-exendin-4 PET/CT, ^{111}In-DOTA-exendin-4 SPECT/CT, and 3T MR imaging for localization of occult insulinomas. Shown is an example from a patient with endogenous hyperinsulinemia hypoglycemia who had a negative endoscopic ultrasound and histology after distal pancreatectomy. A small lesion was seen only retrospectively on the MR image (A) performed previously outside the study as well as on the study MR image (B). It was also negative on ^{111}In-DOTA-exendin-4 SPECT/CT (E,F), but easily visualized on ^{68}Ga-DOTA-exendin-4 PET/CT (C,D). The authors concluded that ^{68}Ga-DOTA-exendin-4 PET/CT should be the diagnostic tool of choice for localization of benign insulinomas when localization fails with contrast-enhanced CT/contrast-enhanced MR imaging.

Readings were blinded and independent and performed by specialists who were not part of the clinical team. The gold standard for all 38 patients was histology. The authors showed that the accuracy and sensitivity of the ^{68}Ga-DOTA-exendin-4 agent were higher than those with the ^{111}In-DOTA SPECT/CT agent as well as than those with MR imaging. In patients who had presented with a prior MR image, the study MR image was more sensitive and accurate than the outside MR image. The study did not include evaluation of negative predictive value or specificity because the patient population was biased with neuroglycopenic symptoms suggesting the presence of an insulinoma. Figure 8 is an example of a patient with endogenous hyperinsulinemia hypoglycemia who had a negative endoscopic ultrasound and histology after distal pancreatectomy. A small lesion was seen only retrospectively on the outside MR image performed prior to the study as well as on the study MR image. ^{111}In-DOTA-exendin-4 SPECT/CT was also negative. Although this is a niche group of patients and a relatively small study, it was well designed with immediate clinically relevant results. The ^{68}Ga agent has been approved for use in Switzerland, where it is reimbursed. The authors were able to carve out a niche area for routine clinical practice, secure both referrals and reimbursement, and have a significant impact on patient care. After resection, many such patients can become asymptomatic and feel much better. The authors concluded that GLP-1R PET/CT should be the diagnostic tool of choice for localization of benign insulinomas when localization fails with contrast-enhanced CT/contrast-enhanced MR imaging.

Two studies from the same institution reported on the results of quality improvement projects related to a challenge we all probably face every day in our PET/CT clinics: radioactivity infiltration at the injection site, resulting in reduced image quality and incorrect quantitation (Fig. 9). Often the arm is extended out of the field of view, so we do not know that this infiltration has occurred, although biodistribution can sometimes provide clues. Townsend et al. from A*STAR-NUS Clinical Imaging Research Centre (Singapore), Duke University (Durham, NC), Lucerno Dynamics, LLC (Cary, NC), the University of North Carolina (Chapel Hill), and other centers reported on "Multicenter assessment of infiltration rates in FDG PET/CT scans: Detection, incidence, and contributing factors" [520]. The group presented a new technology, Lara sensors (Lucerno Dynamics, LLC), that can be placed on the patient's arm. The sensors yield data to derive time–activity curves describing the quality of the injection. The investigators found a range of infiltration rates across multiple PET/CT centers, with an average of 15.2%. This result supports the findings in 7 previously published single-center studies. The results suggest not only that infiltration is common but in many instances may go undetected.

In the second phase of the above study (phase 2) by members of the same consortium, similar assessments were made after initiation of quality improvement plans at 4 PET/CT centers. Wong et al. from A*STAR-NUS Clinical Imaging Research Centre (Singapore), Duke University (Durham, NC), Lucerno Dynamics, LLC (Cary, NC), and the University of North Carolina (Chapel Hill) reported on "Use of a novel detection device to reduce ^{18}F-FDG infiltration rates" [521]. The improvement plans focused on

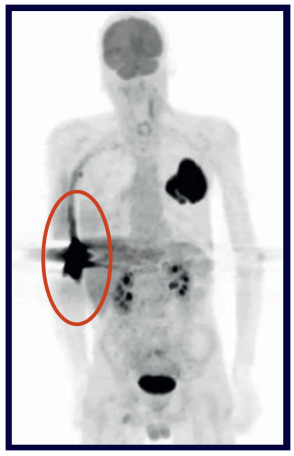

FIGURE 9. Reducing radioactivity infiltration at injection sites in PET/CT. Shown is a typical example of infiltration, which can result in reduced image quality and incorrect quantitation and may go undetected when the injection site is out of the imaging field of view. At the SNMMI meeting, researchers presented a new technology, Lara sensors, that can be placed on the patient's arm to provide data for time–activity curves describing the quality of the injection. These data can, in turn, be used to institute quality improvement measures and reduce the frequency and amount of infiltration.

Downloaded from jnm.snmjournals.org by Ronald Lattanze on February 13, 2020. For personal use only.

factors identified by the Lara technology in the first study, including patient body mass index, weight, age, glucose, injection sites, and orientation. Injection access technique and needle gauge were not associated with differences in infiltration rates. Results varied by adherence to the improvement plans. In the 3 centers that completed the phase 2 study ($n = 830$ injections), the infiltration rate decreased by 51% as compared to phase 1 ($n = 815$ injections). In the fourth center, the infiltration rate decreased by >50%. This new technology is quite interesting. Routine incorporation into a busy clinical center for every patient might be challenging, but this technique could be used to train technologists and other professional staff. It also has important implications for clinical trials, for example in qualifying participating clinical trial sites to improve standardization for quantitation.

Maratto et al. from the Hospital of the University of Pennsylvania and Pennsylvania Hospital (both in Philadelphia) reported on "A hands-free solution to potential cross-contamination in nuclear medicine department restrooms" [1627]. Over the course of 20 days, the authors performed wipe tests on commonly touched areas (door handle, light switch, faucet, soap dispenser, floor, flush handle, and toilet seat) in bathrooms in their nuclear medicine and PET departments. They found that in a median of 4 out of 20 days these counts exceeded 200 counts per minute in 1 or more areas. The investigators took these data to their facilities management and then outfitted several of these areas in their bathrooms with hands-free features. They then reperformed the wipe tests and found that contamination decreased in almost all areas. This is important because, although we are all aware that this contamination happens in the nuclear medicine clinic, the introduction of novel agents and therapies may change the extent and nature of the contamination. This type of information is not only a focus of our interest as nuclear medicine professionals, but a focus for regulatory and public discussion. We can use this and similar quality improvement projects to enhance care for patients, document these efforts, and work collaboratively within our institutional systems.

Conclusion

The themes for the General Nuclear Medicine highlights lecture were efficiency, quantitation, development, and outcomes/quality improvement, and I have profiled representative studies presented at the 2018 SNMMI Annual Meeting. Much of the work presented in general nuclear medicine intersected with SNMMI's Value Initiative in Domain 1: Quality of Practice (including abstracts focused on high-quality, value-driven performance and delivery of patient-centered nuclear medicine) and Domain 2: Research and Discovery. The prospective and retrospective studies presented here are laying promising groundwork for future larger, prospective investigations that can positively impact patient care.

NEWSBRIEFS

NIH-Funded Neighborhood Atlas

The National Institutes of Health (NIH) on June 29 issued a press release describing the availability of the Neighborhood Atlas, a new tool to help researchers visualize socioeconomic data at the community level. This online platform allows for easy ranking and mapping of neighborhoods according to socioeconomic disadvantage, including factors such as income, education, employment, and housing quality. The Neighborhood Atlas is based at the University of Wisconsin (Madison) and was described in the June 28 issue of the *New England Journal of Medicine* (2018;378:2456–2458). The project is funded by the National Institute on Aging and the National Institute on Minority Health and Health Disparities (NIMHD), both part of NIH.

"Socioeconomic disadvantage is 1 of the fundamental factors that result in health disparities, and understanding those factors is what will lead to development of interventions to reduce disparities," said Eliseo J. Pérez-Stable, MD, director of NIMHD. "Having a tool to better understand social factors impacting health disparities is an important step forward to achieving health equity." The atlas was developed by Amy Kind, MD, PhD, from the University of Wisconsin School of Medicine and Public Health, and uses the Area Deprivation Index, which includes 17 measures of education, housing quality, and poverty, updated with current American Community Survey data. Users can download maps indexed with measures of neighborhood disadvantage, ranging from national down to local levels.

The Neighborhood Atlas is built so that it can be merged with other data sources to better understand how neighborhood disadvantage affects health. Dr. Kind noted that the Neighborhood Atlas and its data can be harnessed as a new way to advance disparities-focused research, suggesting that it can be used to improve translational, clinical, and community research by showing ways to aid study design, recruitment, retention, and outreach.

The atlas is already being used by the U.S. Centers for Medicare & Medicaid Services to inform local operations and targeting strategies for the *Everyone with Diabetes Counts* program and to predict the increased likelihood of rehospitalization among individuals in disadvantaged neighborhoods. Access to the atlas is available at https://www.neighborhoodatlas.medicine.wisc.edu/.

National Institutes of Health

Downloaded from jnm.snmjournals.org by Ronald Lattanze on February 13, 2020. For personal use only.

The Journal of NUCLEAR MEDICINE

2018 SNMMI Highlights Lecture: General Nuclear Medicine

Heather A. Jacene

J Nucl Med. 2018;59:7N-13N.

This article and updated information are available at:
http://jnm.snmjournals.org/content/59/10/7N.citation

Information about reproducing figures, tables, or other portions of this article can be found online at:
http://jnm.snmjournals.org/site/misc/permission.xhtml

Information about subscriptions to JNM can be found at:
http://jnm.snmjournals.org/site/subscriptions/online.xhtml

The Journal of Nuclear Medicine is published monthly.
SNMMI | Society of Nuclear Medicine and Molecular Imaging
1850 Samuel Morse Drive, Reston, VA 20190.
(Print ISSN: 0161-5505, Online ISSN: 2159-662X)

© Copyright 2018 SNMMI; all rights reserved.

SNMMI SOCIETY OF NUCLEAR MEDICINE AND MOLECULAR IMAGING